

2) W.G. Love, International Symposium on Light Ion Reaction Mechanisms, Osaka, Japan (1983).

3) W.G. Love and J.R. Comfort, private communication.

4) T.A. Carey et al., Phys. Rev. Lett. 49, 266 (1982).

ENERGY DEPENDENCE OF INELASTIC PROTON SCATTERING TO ONE-PARTICLE ONE-HOLE STATES IN  $^{28}\text{Si}$

C. Olmer, A.D. Bacher, G.T. Emery, W.P. Jones, D.W. Miller, H. Nann, and P. Schwandt  
Indiana University Cyclotron Facility and Physics Department, Bloomington, Indiana 47405

S. Yen, T.E. Drake, and R.J. Sobie  
Department of Physics, University of Toronto, Toronto, Ontario, Canada M5S 1A7

The study of intermediate-energy proton inelastic scattering to one-particle one-hole states is a particularly useful technique for examining selected features of the effective nucleon-nucleon interaction. The structural simplicity of these excited states permits the possible separation of effects due to nuclear structure and those resulting from the reaction mechanism. The present work has concentrated on a study of the energy dependence of proton inelastic scattering for three high-spin, particle-hole states in  $^{28}\text{Si}$ : the  $5^-$ ,  $T=0$  state at 9.70 MeV, the  $6^-$ ,  $T=0$  state at 11.58 MeV, and the  $6^-$ ,  $T=1$  state at 14.35 MeV. Cross-section and analyzing-power measurements for these excitations have been measured at incident proton energies of 80, 100, 134, and 180 MeV, and the data are tabulated in Appendix II, p. 171. The results of this completed study have been recently published;<sup>1</sup> some of the major conclusions of this work are presented here.

A region of the inelastic scattering spectrum measured at 180 MeV is displayed in Fig. 1. Also displayed is a spectrum measured<sup>2</sup> at the same momentum transfer (near the maximum of the cross-section distribution) for an incident proton energy of 800 MeV. The  $6^-$  states are the dominant peaks in the spectrum over the indicated range of excitation energy for the data at 180 MeV, whereas these states are only barely

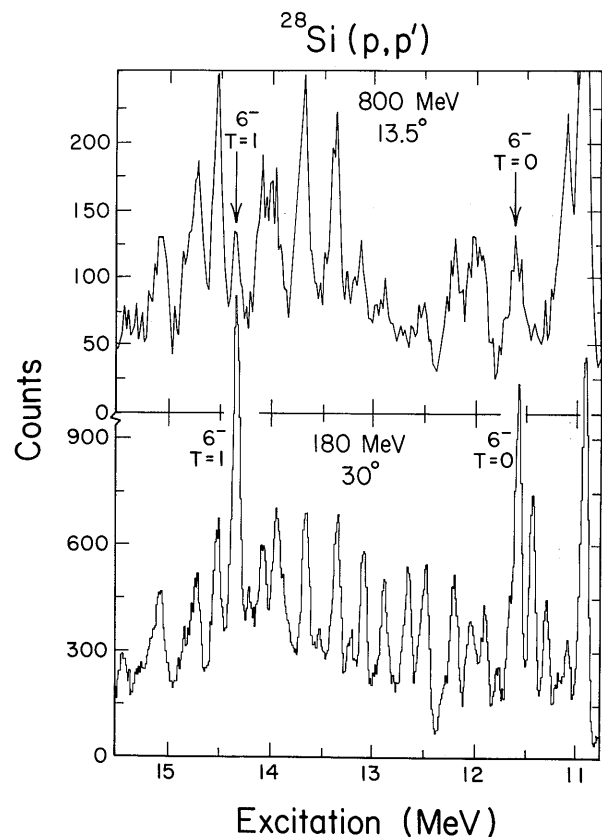


Figure 1. Inelastic proton spectra for the scattering of 180-MeV (bottom) and 800-MeV (top) protons from silicon at similar values of momentum transfer. The 800-MeV data are from Ref. 2.

visible at 800 MeV. This behavior is a consequence of the significant energy dependence of the central, spin-independent term in the effective interaction,

which is primarily responsible for the excitation of neighboring natural-parity states. (A far less severe dependence on energy is indicated for the other components of the effective interaction.) At moderate energies, this term is relatively weak and the excitation of states driven by other terms in the interaction is readily apparent. The strength of this term, however, increases rapidly with energy above about 400 MeV, so that by 800 MeV the unnatural-parity states are obscured by intense neighboring states. As a result, there is a window of proton energies for which detailed inelastic scattering studies of such high-spin states are practical.

The calculation of inelastic scattering within the framework of the distorted-wave impulse approximation (DWIA) requires several essential pieces of information, including a) distortion effects, b) the transition densities of the excitation, and c) an effective nucleon-nucleon interaction.

a) Distortion effects were incorporated in the form of phenomenological Woods-Saxon optical potentials which were derived from simultaneous fits to the elastic scattering cross-section and analyzing-power data which were measured at the four incident energies. The resulting optical-model parameters are presented in Table I. By requiring a smooth dependence on incident energy for these parameters (as well as for the calculated total reaction cross section), a significant reduction in the ambiguity of parameters was possible.

b) The transition form factors for these high-spin states have been assumed to be of harmonic oscillator form, with oscillator parameters deduced in (e,e') studies<sup>3,4</sup> of the 5<sup>-</sup>, T=0 and 6<sup>-</sup>, T=1 transitions (b=1.91 and b=1.743 fm,

TABLE I.  
Optical Model Potential Parameters<sup>a</sup>

	E <sub>p</sub> =80 MeV	100 MeV	134 MeV	180 MeV
V	29.30	25.00	19.30	13.70 MeV
r <sub>o</sub>	1.196	1.229	1.274	1.296 fm
a <sub>o</sub>	0.72	0.72	0.72	0.72 fm
W	5.00	5.50	6.90	13.10 MeV
r <sub>w</sub>	1.521	1.490	1.360	1.128 fm
a <sub>w</sub>	0.346	0.439	0.658	0.715 fm
V <sub>so</sub>	4.42	4.10	3.53	2.80 MeV
r <sub>so</sub>	1.028	1.012	0.955	0.940 fm
a <sub>so</sub>	0.64	0.64	0.64	0.64 fm
W <sub>so</sub>	-0.70	-1.10	-1.80	-2.70 MeV
r <sub>wso</sub>	0.916	0.923	0.935	0.950 fm
a <sub>wso</sub>	0.59	0.59	0.59	0.59 fm
σ <sub>reac</sub>	406	392	374	363 mb

<sup>a</sup>The nuclear optical potential is described by

$$U(r) = -Vf_o(r) - iWf_w(r) + (2.0\text{fm}^2)[V_{so}g_{so}(r) + iW_{so}g_{wso}(r)] \vec{\sigma} \cdot \vec{L}$$

where

$$f_i(r) = [1 + \exp\{(r-r_i A^{1/3})/a_i\}]^{-1}$$

$$g_j(r) = (1/r)(d/dr) [1 + \exp\{(r-r_j A^{1/3})/a_j\}]^{-1}$$

respectively). The 6<sup>-</sup>, T=0 state (unobserved in the (e,e') work) is assumed to have the same oscillator parameter as the 6<sup>-</sup>, T=1 state. Both 6<sup>-</sup> states are characterized by the f<sub>7/2</sub>d<sub>5/2</sub><sup>-1</sup> stretched configuration (the only configuration allowed in a 1 h<sub>w</sub> space). The 5<sup>-</sup>, T=0 state can be described<sup>3</sup> by an RPA excitation operator whose

forward-going part is:

$$\begin{aligned} &+ 0.558f_{7/2}d_{3/2}^{-1} \\ &+ 0.175f_{7/2}d_{5/2}^{-1} \\ &- 0.121f_{5/2}d_{5/2}^{-1} \end{aligned}$$

with backward-going terms 0.050, -0.041 and -0.046, respectively. The calculations for the  $6^-$  transitions assume a filled  $d_{5/2}$  shell in the ground state; deviations from this assumption are expected and will be reflected in the resulting normalization factors.

c) Several different free and density-dependent prescriptions of the effective nucleon-nucleon interaction have been examined in this study.

These include:

- (i) the Love-Franey interaction<sup>5</sup> (LF), a free interaction based on a parameterization of the free nucleon-nucleon  $t$ -matrix at several energies.
- (ii) the Paris free interaction<sup>6</sup> (PF), a free interaction based on the Paris nucleon-nucleon potential.<sup>7</sup>
- (iii) the Paris density-dependent interaction<sup>6</sup> (PDD), a density-dependent interaction derived using the underlying Paris nucleon-nucleon potential<sup>7</sup> and several different values of the nuclear matter density.
- (iv) the Picklesimer-Walker interaction<sup>8</sup> (PW), an energy-independent free interaction which explicitly incorporates both energy and momentum dependence.
- (v) the Hamada-Johnston interaction<sup>9</sup> (HJ), a density-dependent interaction derived using the underlying Hamada-Johnston nucleon-nucleon potential<sup>10</sup> and several

different values of the nuclear matter density.

The DWIA calculations using the LF and PW interactions were carried out with the code DW81.<sup>11</sup> The calculations using the PF, PDD, and HJ interactions were carried out with the code DWBA70<sup>12</sup>, modified to include possible density dependence. All calculations treated the exchange term in an exact manner.

A conceptually simple comparison of the DWIA predictions with the data involves the energy dependence of the maximum cross section  $\sigma_{\max}$ , since such a comparison is independent of momentum transfer. Displayed in Fig. 2 are the renormalization factors which are required in order for the theoretical values of  $\sigma_{\max}$  to reproduce the experimental values at each incident energy. Ideally, the value of the renormalization factor should be independent of beam energy, with a value characteristic of the nuclear structure of the excited state.

For the  $5^-$ ,  $T=0$  transition, the renormalization factors for all of the indicated interactions exhibit similar values and a relatively flat energy dependence (with the exception of the PW interaction at 180 MeV). As a result of these observations, it may be concluded the LF, PDD, and PF interactions reproduce reasonably well the energy dependence of  $\sigma_{\max}$  for the  $5^-$  transition. An average of the renormalization factors at 100, 134, and 180 MeV results in values of 0.645 for the LF interaction, 0.64 for the PF interaction, 0.63 for the PDD interaction, and 0.69 for the PW interaction. None of these factors reproduces the value deduced<sup>3</sup> in the  $(e,e')$  studies (approximately 0.92). Possible sources of this discrepancy are considered in Ref. 1.

The renormalization factors deduced for the  $6^-$ ,  $T=0$  transition in DWIA analyses using the various

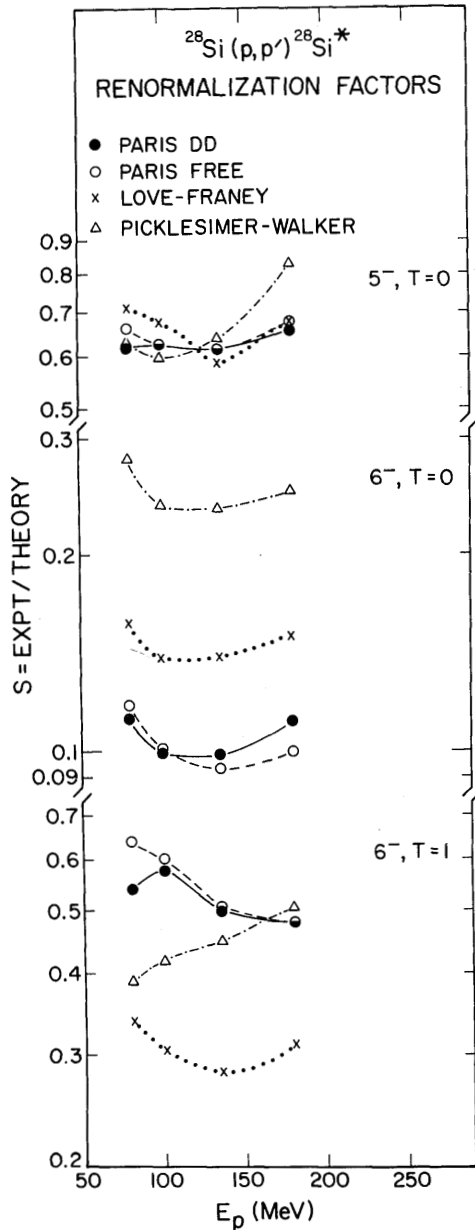


Figure 2. Energy dependence of the renormalization factors for inelastic proton excitation of the  $5^-, T=0$ ,  $6^-, T=0$  and  $6^-, T=1$  states in  $^{28}\text{Si}$ . The experimental values of the maximum cross section are divided by the theoretical values for the various indicated effective interactions.

effective interactions exhibit a similar energy-dependent behavior over the indicated energy range. However, rather different values of these factors are observed for different interactions. An

average of the renormalization factors at 100, 134, and 180 MeV results in values of 0.143 for the LF interaction, 0.099 for the PF interaction, 0.103 for the PDD interaction and 0.241 for the PW interaction.

For the  $6^-, T=1$  transition, the renormalization factors extracted for the various effective interactions display rather different magnitudes as well as a significant dependence on incident energy. The LF results decrease in magnitude by 20% from 80 to 134 MeV, where the renormalization factor equals 0.28, and then increase by 10% from 134 to 180 MeV. The PW results systematically increase with increasing energy, and a value of 0.45 is observed at 134 MeV. Although different in magnitude at 80 MeV, the PF and PDD results are very similar at the other energies and decrease in value from 100 to 180 MeV, with a value of  $\sim 0.5$  observed at 134 MeV. An average of the renormalization factors at 100, 134 and 180 MeV results in values of 0.30 for the LF interaction, 0.53 for the PF interaction, 0.52 for the PDD interaction and 0.46 for the PW interaction.

The observation of renormalization factors substantially less than one for both the  $6^-, T=0$  and  $6^-, T=1$  transitions can be a consequence of several different factors. First, the nuclear structure assumptions in these calculations may not be fully correct. The assumption of an  $f_{7/2}$  excitation from a filled  $d_{5/2}$  shell is too simplistic; a more realistic model would include the depletion in strength of this particle-hole configuration (see, e.g., Ref. 3). In addition, the strength and energy dependence of the force components responsible for these transitions may not be well determined. Certainly the observation of an energy-dependent behavior for the renormalization factors suggests that the energy dependence of the relevant force components may be incorrect. In order to

investigate these various possibilities, it is instructive to also examine the results for inelastic electron and pion scattering, since the inelastic excitation of stretched unnatural-parity states by all three probes should be sensitive to the same transition form factors.<sup>13</sup>

A recent distorted-wave analysis<sup>4</sup> of the  $(e, e')$  data<sup>3</sup> for the  $6^-$ ,  $T=1$  transition results in a value of 0.366 which should be directly comparable to the values extracted in the  $(p, p')$  and  $(\pi, \pi')$  studies. Analyses<sup>14</sup> of the inelastic pion scattering data at 162 MeV indicate that renormalization factors of 0.13 and 0.34 are required for the  $6^-$ ,  $T=0$  and  $6^-$ ,  $T=1$  transitions, respectively, when harmonic-oscillator form factors and a pure  $f_{7/2} d_{5/2}^{-1}$  configuration are employed in the distorted-wave calculations. For inelastic proton scattering, no single effective interaction reproduces the electron scattering result over the entire proton energy range. However, calculations using the LF interaction are in very close agreement with both the electron-deduced and pion-deduced values.

The relative excitation of the  $6^-$  isoscalar and isovector transitions is displayed in Fig. 3. In the upper portion of the figure, the experimental and theoretical ratios of the maximum cross sections for the  $6^-$ ,  $T=0$  and  $6^-$ ,  $T=1$  transitions are indicated for inelastic proton and pion scattering. The theoretical ratios for  $(p, p')$  are labelled by the appropriate effective interaction used in the DWIA calculations; the theoretical ratio for  $(\pi, \pi')$  is discussed in detail in Ref. 14. These theoretical ratios are divided by the experimental ratios and are presented in the lower portion of Fig. 3. (Note that this final ratio is also equivalent to  $S_1/S_0$ , where  $S_1$  and  $S_0$  are the renormalization factors for the  $6^-$ ,  $T=1$  and  $6^-$ ,  $T=0$

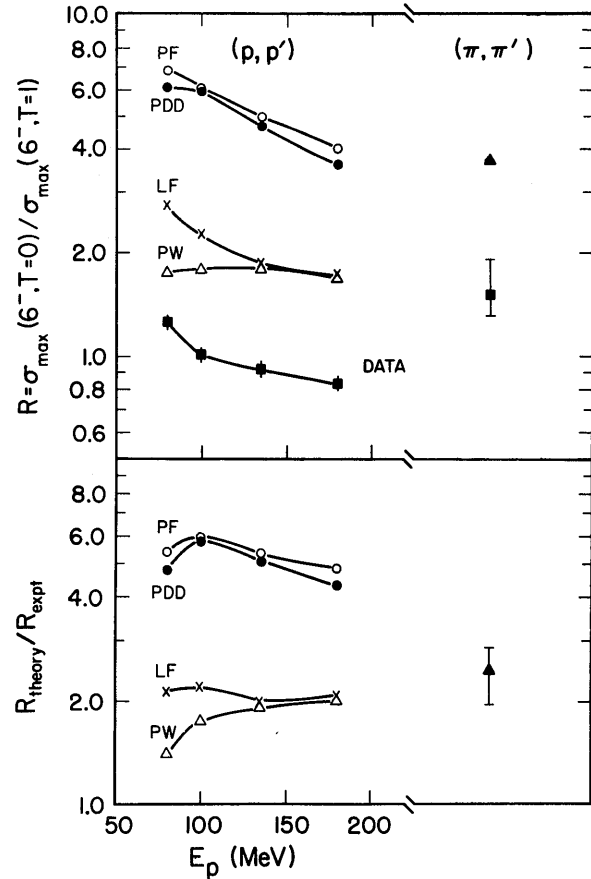


Figure 3. Energy dependence of the relative strengths for the  $6^-$ ,  $T=0$  and  $6^-$ ,  $T=1$  excitations. Top: Ratio of maximum cross sections  $\sigma_{\max}(6^-, T=0)/\sigma_{\max}(6^-, T=1)$  observed in inelastic proton and inelastic pion scattering, together with DWIA predictions discussed in the text. The experimental values of  $R$  are indicated by the solid squares. Bottom: Ratio of theoretical predictions and experimental values displayed in the top part.

transitions, respectively, deduced by dividing the experimental maximum cross section by the theoretical maximum cross section. If the strengths of the isoscalar and isovector interactions are correctly described, then this ratio can be interpreted as the ratio of spectroscopic factors for the two transitions.)

The theoretical ratios of isoscalar to isovector cross sections shown in the top of Fig. 3 for the PF, LF and PDD interactions, as well as the experimental ratio, all exhibit a decrease in magnitude with

increasing incident energy, whereas the PW ratios do not demonstrate this decrease. In particular, the energy dependence of the LF predictions is very similar to the experimental observations (see bottom of Fig. 3). The energy dependences predicted by the PF and PDD calculations are larger than the experimental observations, while a weaker energy dependence is predicted by the PW calculations. In addition to displaying the desired dependence on energy, the DWIA calculations using the LF interaction also predict an average ratio of renormalization factors  $S_1/S_0$  ( $\sim 2.10$ ) which is rather similar to that deduced<sup>14</sup> in the  $(\pi, \pi')$  analyses (2.47<sup>+0.38</sup><sub>-.52</sub>).

The most important conclusion based on an examination of the  $(p, p')$  results displayed in Figs. 2 and 3 is the observation of significantly different renormalization factors extracted for the  $6^-$ ,  $T=0$  and  $6^-$ ,  $T=1$  states, as well as quite different ratios of strengths deduced for these transitions resulting from the DWIA calculations using the various forms of the effective interaction. These two transitions are sensitive to different components of the effective interaction which are specified in different ways by the theoretical groups that have constructed these various forms of the interaction. If the unambiguous extraction of nuclear structure information using inelastic proton scattering is to be a viable technique, then there must be some independent way of selecting one particular form of the interaction as a better representation than the others.

A more rigorous test of the various forms of the effective interaction is provided by a detailed examination of the energy and momentum-transfer dependence of the cross section and analyzing power. Comparisons of the DWIA predictions (using the different interactions) with the experimental results

are presented and discussed in detail in Ref. 1. Here, we present a few representative cases.

The cross-section distributions measured for the  $5^-$ ,  $T=0$  transition at the four incident energies are displayed as a function of momentum transfer in Figs. 4-5, together with DWIA calculations employing the LF and PF effective interactions and optical model parameters appropriate for the different energies. The decomposition of the predicted cross section into central (C), spin-orbit (LS) and tensor (T) contributions is indicated for each of the various

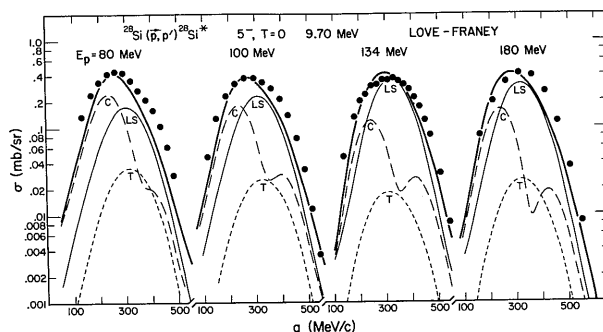


Figure 4. Momentum-transfer dependence of the cross sections for inelastic proton excitation of the  $5^-$ ,  $T=0$  state in  $^{28}\text{Si}$ . The curves are DWIA calculations (multiplied by 0.667) using the Love-Franey effective interaction and optical potentials appropriate for the various energies.

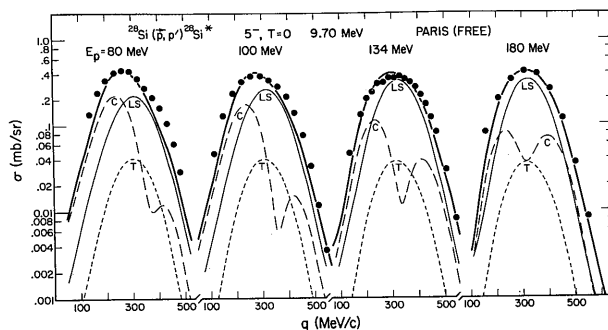


Figure 5. Momentum-transfer dependence of the cross sections for inelastic proton excitation of the  $5^-$ ,  $T=0$  state in  $^{28}\text{Si}$ . The curves are DWIA calculations (multiplied by 0.667) using the free Paris effective interaction and optical potentials appropriate for the various energies.

interactions. For display purposes, these calculations have been arbitrarily normalized to the data at 180 MeV; the resulting multiplicative factors are specified in the individual figure captions.

Calculations using the LF interaction appear to reproduce the energy dependence of  $\sigma_{\max}$  reasonably well, while somewhat worse agreement is seen for the energy dependence of  $q_{\max}$  (the location of  $\sigma_{\max}$ ). However, a detailed inspection of the entire momentum-transfer dependence reveals that these calculations consistently fail to reproduce the width of the experimental distributions. The predicted distributions are narrower than experimentally observed and, moreover, the calculations do not exhibit the observed increase in width of the distributions at the lower incident energies.

As shown in Fig. 5, calculations using the PF interaction reproduce extremely well the energy dependences of  $\sigma_{\max}$  and  $q_{\max}$ , as well as the experimental widths of the distributions. In particular, the shapes of the distributions at 135 and 180 MeV are poorly reproduced beyond  $q \sim 300$  MeV/c for the LF calculations, whereas excellent agreement is observed for the PF calculations. Only very small differences are seen between the PDD and PF calculations, thereby indicating that density-dependent effects are not significant for explaining the cross section, as is expected from the surface nature of this high-spin transition. Rather, a detailed comparison of the results for the two free interactions (LF and PF) indicates that the major factor in explaining the data is the large, second maximum of the central component in the PF (and PDD) calculations, which is very weak in the LF calculations. Even though all these calculations show the spin-orbit component to be dominant for the  $5^-$  cross section over a large range of

momentum transfer, and the magnitude as well as the momentum-transfer dependence of the spin-orbit contribution to the cross section are very similar for these interactions at the four incident energies, it is, in fact, the different description of the central component in the Paris framework which produces excellent agreement with the data. It is important to note that conclusions regarding the importance of density-dependent effects which result from a comparison of calculations using free and density-dependent interactions of different families (e.g. LF and PDD) can be extremely misleading or incorrect.

The cross-section distributions measured for the  $6^-$ ,  $T=1$  transitions are displayed in Figs. 6 and 7, together with DWIA calculations using the LF and PF interactions. These calculations are arbitrarily normalized to the data at 180 MeV, with the resulting factors specified in the individual figure captions. All of these calculations indicate that this transition occurs predominantly through the tensor component of the interaction, although the central and spin-orbit components

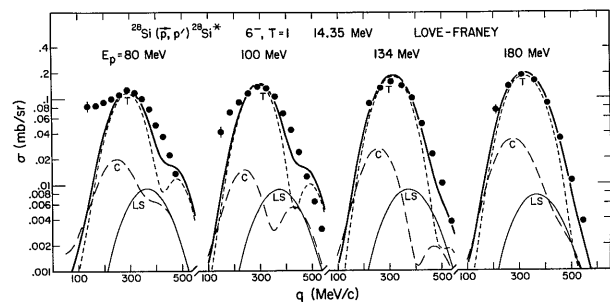


Figure 6. Momentum-transfer dependence of the cross sections for inelastic proton excitation of the  $6^-$ ,  $T=1$  state in  $^{28}\text{Si}$ . The curves are DWIA calculations (multiplied by 0.30) using the Love-Franeay effective interaction and optical potentials appropriate for the various energies.

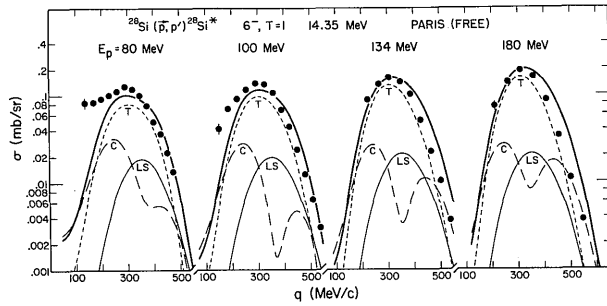


Figure 7. Momentum-transfer dependence of the cross sections for inelastic proton excitation of the  $6^-$ ,  $T=1$  state in  $^{28}\text{Si}$ . The curves are DWIA calculations (multiplied by 0.50) using the free Paris effective interaction and optical potentials appropriate for the various energies.

certainly affect the overall shapes of the distributions. (Note that we are now examining the isovector components of the interaction, rather than the isoscalar components relevant for the  $5^-$ ,  $T=0$  and  $6^-$ ,  $T=0$  transitions).

The calculations using the LF interaction better reproduce the energy dependence of  $\sigma_{\text{max}}$  and  $q_{\text{max}}$ , as well as the momentum transfer dependence of the data at the higher energies. The different widths of the distributions predicted by the LF and PF calculations at 134 and 180 MeV are a consequence of the different descriptions of the central components of the two interactions since very similar tensor contributions are observed, whereas the central contributions exhibit very different dependences on momentum transfer. As expected, a comparison of the PF and PDD results indicates that the effect of density dependence is not important in a calculation of the cross section for this transition.

The experimental analyzing-power distributions for the  $5^-$ ,  $T=0$  and  $6^-$ ,  $T=1$  transitions at the four incident energies are shown in Figs. 8 and 9, together with predictions based on the various forms of the effective nucleon-nucleon interaction. Since the

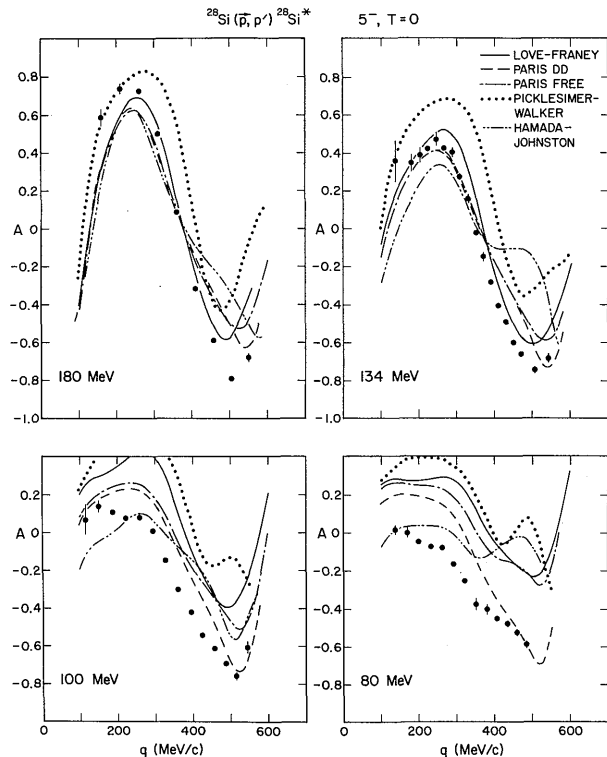


Figure 8. Momentum-transfer dependence of the analyzing powers for inelastic proton excitation of the  $5^-$ ,  $T=0$  state. The curves are DWIA calculations discussed in the text.

analyzing power is a direct result of the interference of amplitudes, a comparison of the predicted and observed analyzing powers provides an independent test of the interaction, separate from that furnished by the cross section. Moreover, the interference nature of the analyzing power suggests that possible density-dependent effects may be manifested in a quite different manner than observed in an analysis of the cross-section results.

The  $5^-$ ,  $T=0$  analyzing-power data shown in Fig. 8 exhibit a general trend of a positive (or near zero) value at small momentum transfer, followed by a decrease towards strongly negative values with increasing momentum transfer. As the incident proton



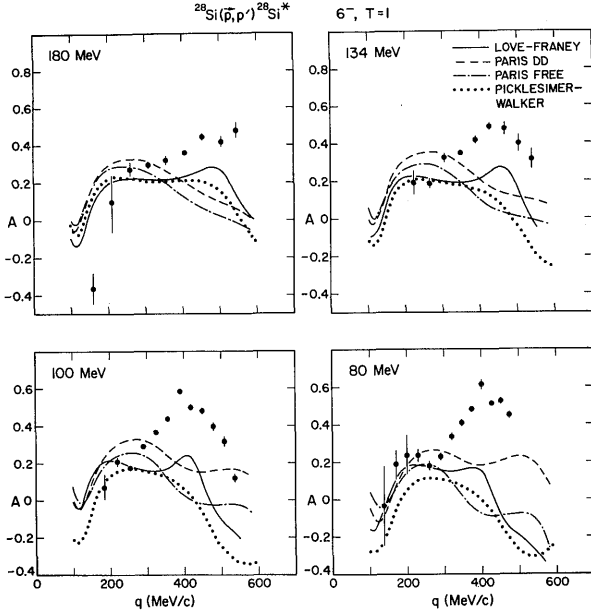


Figure 9. Momentum-transfer dependence of the analyzing powers for inelastic proton excitation of the  $6^-$ ,  $T=1$  state. The curves are DWIA calculations discussed in the text.

energy increases, the most positive value of the analyzing power increases (from near zero at 80 MeV to  $\sim 0.7$  at 180 MeV) and the location where the analyzing power crosses zero moves to larger momentum transfer (from  $\sim 200$  MeV/c at 80 MeV to  $\sim 370$  MeV/c at 180 MeV). Some of these qualitative features can be generally understood from a consideration<sup>15</sup> of the plane-wave impulse approximation (PWIA) expression for the analyzing power of the  $5^-$  transition,

$$A(q) = \frac{2t_R^{LS}t_I^C - 2t_I^{LS}t_R^C}{|t^C|^2 + |t^{LS}|^2}, \quad (1)$$

where magnetization and current contributions are neglected. Here  $t^C$  and  $t^{LS}$  are the spin-independent central and spin-orbit terms in the effective interaction, and the expression in the denominator of Eq. (1) corresponds to the predicted cross section within this framework. The interference nature of the

analyzing power is readily apparent from an inspection of Eq. (1). The zero-crossing feature of the  $5^-$  analyzing power is associated with a change in sign of  $t_R^C$  and  $t_I^C$  (the real and imaginary parts of  $t^C$ ) over the range of momentum transfer under consideration. A direct consequence of this change in sign of the central terms is the two-lobed character of the central contribution to the  $5^-$  cross section (see, for example, Fig. 4).

The predicted analyzing-power distributions displayed in Fig. 8 for distorted-wave calculations using the various interactions all exhibit the qualitative increase in the most positive value of the analyzing power as the bombarding energy increases. On the other hand, the predicted location of the zero crossing changes only slightly with energy, in contrast to the rather large dependence observed in the data. The LF, PF and PDD calculations are all in reasonable agreement with the data at the higher energies, whereas the PDD interaction is preferred at the lower energies, where a comparison of the PF and PDD calculations indicates the effect of density dependence on the analyzing power to be most pronounced. The influence of distortion on these calculations is principally to affect the location of the zero crossing; the PWIA calculations predict relatively large analyzing powers for the  $5^-$  transition at the higher bombarding energies.

The  $6^-$ ,  $T=0$  and  $T=1$  excitations are both unnatural-parity transitions of stretched nature and, as a result, the analyzing power in the PWIA is given by<sup>15</sup>

$$A(q) = \frac{2t_R^{LS}(t_I^C + t_I^{T\beta}) - 2t_I^{LS}(t_R^C + t_R^{T\beta})}{|t^C + t^{T\alpha}|^2 + |t^{LS}|^2 + |t^C + t^{T\beta}|^2 + \zeta^* |t^C + t^{T\gamma}|^2} \quad (2)$$

where  $t^{T\alpha}$ ,  $t^{T\beta}$  and  $t^{T\gamma}$  are three different linear

combinations of the direct and exchange tensor terms,  $t^C$  refers here to the spin-dependent central force, and  $\zeta = 2J/(J + 1)$ . It is apparent from Eq. (2) that the analyzing power for such transitions provides information on the interference between the spin-orbit term on the one hand, and both the tensor and central terms of the effective interaction on the other hand, whereas the cross section is sensitive to the interference only between the central and tensor terms in the interaction. The analyzing powers for these two transitions predicted by the PWIA are generally quite small, in contrast to the experimental observation of moderately large values over the entire energy range. The influence of distortions on these calculations is to increase significantly the predicted values of the analyzing power. This is a consequence of a term in  $|t_R^T|^2$  which, in the presence of spin-orbit distortion, has a large contribution to the analyzing power but which is not present in the PWIA.

The analyzing-power data for  $6^-$ ,  $T=1$  transition shown in Fig. 9 show distributions peaked at relatively large momentum transfer ( $\sim 400$  MeV/c) at all incident energies. This general trend is also present in the LF calculations, although the predicted magnitude of the rise at large momentum transfer is too small. Although neither the PF nor the PDD calculations provide good agreement with the data, a comparison of these calculations suggests that the apparent effect of density dependence is to increase the analyzing power at large momentum transfer, and a relatively large effect is seen at the lower energies. The implementation of density dependence within the LF framework would be a promising direction to pursue.

These conclusions regarding the relative success and failure of the various interactions to reproduce the analyzing-power data for the three transitions need

to be considered together with the previous discussion regarding the cross-section analyses. Although the cross-section and analyzing-power observables are, in principle, sensitive to quite different combinations of the interaction components, the difficulties encountered in explaining the cross-section results for the  $6^-$  transitions very likely also affect in some manner the quality of the agreement for the analyzing-power calculations. On the whole, however, the general success in reproducing the qualitative features of the analyzing-power data for all three transitions over the indicated ranges of bombarding energy and momentum transfer is most encouraging, particularly taking into account the large sensitivity to distortion effects expected for the  $6^-$ ,  $T=0$  and  $6^-$ ,  $T=1$  transitions.

- 1) C. Olmer, A.D. Bacher, G.T. Emery, W.P. Jones, D.W. Miller, H. Mann, P. Schwandt, S. Yen, T.E. Drake and R.J. Sobie, Phys. Rev. C 29, 361 (1984).
- 2) N. Hintz, private communication.
- 3) S. Yen, R.J. Sobie, H. Zarek, B.O. Pich, T.E. Drake, C.F. Williamson, S. Kowalski, and C.P. Sargent, Phys. Lett. 93B, 250 (1980); S. Yen, R.J. Sobie, T.E. Drake, H. Zarek, C.F. Williamson, S. Kowalski and C.P. Sargent, Phys. Rev. C 27, 1939 (1983); S. Yen, Ph.D. Thesis, University of Toronto (1983).
- 4) R.A. Lindgren, private communication.
- 5) W.G. Love and M.A. Franey, Phys. Rev. C 24, 1073 (1981).
- 6) H.V. von Geramb and K. Nakano, in The Interaction Between Medium Energy Nucleons in Nuclei-1982, edited by H.O. Meyer (AIP Conf. Proc. No. 97, New York, 1983), p.44.
- 7) M. Lacombe, B. Loiseau, J.M. Richard, R. Vinh Mau, J. Côté, P. Pires and R. de Tourreil, Phys. Rev. C 21, 861 (1980).
- 8) A. Picklesimer and G.E. Walker, Phys. Rev. C 17, 237 (1978).
- 9) H.V. von Geramb, Table of Effective Density and Energy Dependent Interactions for Nucleons, Part A: Central Potential; W. Bauhoff and H.V. von Geramb, Part B: Spin-Orbit Potential, preprint, Universitat Hamburg (1980).
- 10) T. Hamada and I.D. Johnston, Nucl. Phys. 34, 382 (1962).

- 11) R. Schaeffer and J. Raynal, Saclay Report CEA-R4000 (1970); modified by J. Comfort.
- 12) R. Schaeffer and J. Raynal, Saclay Report CEA-R4000 (1970); modified by W. Bauhoff.
- 13) F. Petrovich and W.G. Love, Proc. of the International Conference on Nuclear Physics, Berkeley, California (1980), edited by R.M. Diamond and J.D. Rasmussen, Nucl. Phys. A354, 499C (1981).
- 14) C. Olmer, B. Zeidman, D.F. Geesaman, T.-S. H. Lee, R.E. Segel, L.W. Swenson, R.L. Boudrie, G.S. Blanpied, H.A. Thiessen, C.L. Morris, and R.E. Anderson, Phys. Rev. Lett. 43, 612 (1979).
- 15) S. Yen, R.J. Sobie, T.E. Drake, A.D. Bacher, G.T. Emery, W.P. Jones, D.W. Miller, C. Olmer, P. Schwandt, W.G. Love, and F. Petrovich, Phys. Lett. 105B, 421 (1981).

ELASTIC SCATTERING OF 100 MeV POLARIZED PROTONS FROM  $^4\text{He}$

A. Nadasen

University of Michigan, Dearborn, Michigan 48128

P.G. Roos, D. Mack, G. Ciangaru, and L. Rees

University of Maryland, College Park, Maryland 20742

P. Schwandt and K. Kwiatkowski

Indiana University Cyclotron Facility, Bloomington, Indiana 47405

R.E. Warner

Oberlin College, Oberlin, Ohio 44074

A.A. Cowley

CSIR, Faure, South Africa

The interaction between few-nucleon systems is of considerable interest to both theorists and experimentalists because (1) a limited number of nucleons are involved, (2) very few reaction channels are open, and (3) multiple scattering is greatly reduced. Thus it is possible to carry out fundamental calculations in terms of basic nucleon-nucleon forces, e.g. in the framework of resonating group theory, three-body cluster models utilizing Fadeev equations, or a coupled reaction channel formalism. Such calculations also provide a means for the direct evaluation of different prescriptions for the nucleon-nucleon interaction.

The success of such studies in providing a more complete understanding of nuclear reactions rests on the availability of a large body of accurate experimental data on few-nucleon systems, including elastic scattering as well as reaction data. For the p +  $^4\text{He}$  system, data of good quality are available for

elastic scattering in the form of differential cross sections and analyzing powers up to 65 MeV<sup>1</sup> and in the 200 to 500 MeV range.<sup>2</sup> These measurements show characteristic qualitative differences between the lower-energy data and the higher-energy data. The differential cross sections at the lower energies exhibit strong backward peaking, presumably due to coupled-channel or exchange effects, in contrast to the higher-energy data. Up to 65 MeV, the analyzing powers are generally small in the forward hemisphere, with a moderate negative swing around 100° followed by a large positive maximum near 140°. For proton energies beyond 200 MeV, on the other hand, one observes strong oscillations of the analyzing powers in the forward hemisphere, with peak values decreasing with increasing energy [ $\approx \pm 1$  at 200 MeV to  $\approx \pm 0.5$  at 500 MeV]. In the backward hemisphere the analyzing powers are predominantly negative.

In response to the paucity of high-quality data in